Computational and Structural Biotechnology Journal 27 (2025) 1383–1393

Contents lists available at ScienceDirect

Computational and Structural Biotechnology Journal

journal homepage: www.elsevier.com/locate/csbj

Research Article

LncRNA-miRNA interplay regulate intestinal regeneration in the sea cucumber *Apostichopus japonicus*

Fang Su [a,b,c,d], Igor Yu. Dolmatov [e], Tianming Wang [f], Hongsheng Yang [a,b,c,d], Kui Ding [a], Libin Zhang [a,b,c,d], Lina Sun [a,b,c,d,*]

[a] CAS Key Laboratory of Marine Ecology and Environmental Sciences, Institute of Oceanology, Chinese Academy of Sciences, Qingdao 266071, China
[b] Laboratory for Marine Ecology and Environmental Science, Qingdao Marine Science and Technology Center, Qingdao 266237, China
[c] Key Laboratory of Breeding Biotechnology and Sustainable Aquaculture (CAS), Institute of Oceanology, Chinese Academy of Sciences, Qingdao 266071, China
[d] University of Chinese Academy of Sciences, Beijing 100049, China
[e] A.V. Zhirmunsky National Scientific Center of Marine Biology, Far Eastern Branch, Russian Academy of Sciences, Vladivostok 690041, Russia
[f] National Engineering Laboratory of Marine Germplasm Resources Exploration and Utilization, Marine Science and Technology College, Zhejiang Ocean University, Zhoushan 316022, China

ARTICLE INFO

Keywords:
Long non-coding RNA (lncRNA)
Intestinal regeneration
Echinoderm
Apostichopus japonicus

ABSTRACT

The sea cucumber *Apostichopus japonicus*, renowned for its remarkable ability to expel and regenerate its internal organs within weeks, serves as a model organism for regeneration research. However, studies on the role of non-coding RNAs, particularly long non-coding RNA (lncRNA), in intestinal regeneration remain limited. In this study, we identified and performed differential expression analysis of lncRNAs in both normal intestines and intestines at 3 days post evisceration (dpe). A total of 2361 lncRNAs were identified, 183 of which were differentially expressed (DE-lncRNAs). The genes targeted by these lncRNAs, either cis- or trans-acting, were involved in oxidative stress, immune response, extracellular matrix remodeling, and energy metabolism during intestinal regeneration. Notably, MSTRG.6200/miR-7847–3p and MSTRG.18440/miR-4220–5p have been confirmed as interacting lncRNA-miRNA pairs. These results suggest that lncRNAs are key regulators of intestinal regeneration in *A. japonicus*, offering new insights into the underlying mechanisms and potential targets for enhancing regeneration.

1. Introduction

In the realm of marine biodiversity, echinoderms represent a large phylum of deuterostome invertebrates sharing a common ancestor with chordates [1]. Echinoderms occupy a pivotal position within evolutionarily lineage, offering critical insights into developmental and evolutionary processes. A particularly intriguing biological feature of these animals is their capacity for autotomy and regeneration, traits likely present since the Ordovician and inherited from stem-group echinoderms [2]. Holothurians or sea cucumbers represent the evolutionarily youngest class of echinoderms. Due to their unique developmental position and rapid regenerative capabilities, holothurians have emerged as model organisms for regeneration research. Evisceration involves removing the intestine and some other organs under predation risk or environmental stress [3]. The phenomenon of evisceration and regeneration in holothurians has been documented since the mid-19th century [4]. To date, numerous reviews have summarized progress across tissue, cellular, and molecular levels [5–9].

The sea cucumber *Apostichopus japonicus* (Echinodermata, Holothuroidea, Synallactida, *Apostichopus*) expels most internal organs (intestine, respiratory trees, gonad tubules) through the cloaca and complete regeneration within three weeks [10,11]. Intestinal regeneration begins at the free end of the remaining mesentery, the esophagus remnant and cloaca [9]. Many studies focus on the role of the mesentery in this process [12,13]. Indeed, morphologically, wound healing and the initiation of regeneration commence simultaneously at the mesentery and esophagus remnant. Despite the lack of definitive evidence for stem cells involved during intestinal regeneration in echinoderms [4], their remarkable regenerative abilities are likely attributed to the coelomic epithelial cells' capacity for dedifferentiation and transdifferentiation

* Corresponding author at: CAS Key Laboratory of Marine Ecology and Environmental Sciences, Institute of Oceanology, Chinese Academy of Sciences, Qingdao 266071, China.
E-mail address: sunlina@qdio.ac.cn (L. Sun).

https://doi.org/10.1016/j.csbj.2025.03.047
Received 20 January 2025; Received in revised form 19 March 2025; Accepted 28 March 2025
Available online 31 March 2025

[14]. At approximately 3 days post-evisceration (3 dpe), the residual tubular esophagus closes and connects to the mesentery, forming a blind tubular outgrowth [15]. Simultaneously, connective tissue thickenings, referred to as " anterior gut anlagen", emerge at blind tubular outgrowths, forming the basis for the future intestine. These events highlight the complexity and coordination involved in holothurian regeneration. Significant cell proliferation and apoptosis were observed in the intestine at 3dpe [16]. Differentially expressed genes were primarily localized to extracellular regions and involved in cell adhesion processes. These genes were significantly enriched in functional terms including peptidase/enzyme regulatory activity, inhibitor activity, and signaling receptor binding. A pronounced material reorganization process occurs during this phase, with multiple signaling pathways related to protein degradation being significantly enriched, including lysosomal signaling pathway, autophagy signaling pathway, mitophagy signaling pathway, and FoxO signaling pathway. Moreover, mucin-type O-glycan biosynthesis and other types of O-glycan biosynthesis signaling pathways, which play a crucial role in modulating cell adhesion and recognition as well as influencing cell signaling and interactions, were also significantly enriched [16]. In summary, extensive extracellular and intercellular interactions occurr at 3dpe.

To elucidate the molecular mechanisms underlying regeneration, a comprehensive analysis of regulatory networks is critical. Beyond mRNA-mediated regulation, non-coding RNAs (ncRNAs) have emerged as a pivotal player at the levels of transcription, RNA processing, and translation [17]. Utilizing the high-quality genome of *A. japonicus* [18,19], the expression profiles of circRNA and microRNA during intestinal regeneration have been elucidated, revealing their involvement in signaling transduction, cell proliferation, migration, and other cellular events [20,21]. However, studies on the regulation of long non-coding RNA (lncRNA) in intestinal regeneration are still limited. LncRNAs, which exceed 200 nucleotides in length, account for over 80 % of non-coding RNAs, representing a major functional category. They were previously regarded as junk RNA or transcriptional noise; however, increasing research indicates that they play significant roles in various biological processes, such as immune response and development, in both vertebrates and invertebrates [22–26]. In the field of animal regeneration, lncRNA *CR40469* is essential for wing regeneration in *Drosophila*, although it is not necessary for imaginal disc development [27]. Furthermore, lncRNA SNHG1 promotes cartilage regeneration [28] and lncRNA CASC11 regulates the progress of delayed fracture healing via sponging miR-150–3p [29]. LncRNAs play an instrumental role in regulating intestinal stem cells, intestinal homeostasis, and regeneration [30], e.g., lncRNA CR46040, which is essential for injury-stimulated regeneration of intestinal stem cells in *Drosophila* [31], and the lncRNA H19, whose level is increased by interleukin 22 signaling in inflamed intestinal tissues and epithelial cells and which promotes mucosal regeneration [32].

In the physiology of aquaculture animals, lncRNAs are involved in reproduction, immune response, growth and development, environmental response processes, and basic life activities such as pigmentation, metabolism, and biological rhythm [33]. Given the low conservation of lncRNAs across species [34], functional studies in diverse taxa are essential to uncover common patterns of these molecules in biological processes. In the present study, we employed RNA sequencing technology to identify lncRNAs and their differential expression in the regenerating (3dpe) and normal intestines of *A. japonicus*. We also aimed to confirm the interaction between lncRNAs and microRNAs in gene expression regulation using dual-luciferase reporter assays. Our extensive research on regeneration of *A. japonicus*, combined with the identification of lncRNAs, not only lays the foundation for further investigation into lncRNA-mediated animal regeneration mechanisms but also provides fascinating insights for exploration in regenerative medicine.

2. Material and methods

2.1. Sample collection

The experimental sea cucumbers *A. japonicus* (70–100 g) were purchased from Shandong Oriental Ocean Sci-Tech Co., Ltd. Shandong Province, China and subsequently acclimated in culture tanks at a temperature of approximately 18 °C for two weeks. Animals were fed daily, and feces were removed to maintain intestinal health. To induce evisceration, 3–5 mL of 0.35 M KCl solution was injected into the coelom [20]. The time of evisceration was assumed to be the starting point of regeneration. Three regenerated intestines were collected at 3dpe. The normal intestines were used as the control group. After the intestines were dissected, they were immediately frozen in liquid nitrogen.

2.2. RNA extraction, library construction and sequencing

Total RNA was extracted using Trizol reagent (Invitrogen, CA, USA) following the manufacturer's protocol. Quality control of total RNA was carried out through quantification by Nanodrop and detection of RNA integrity by Agilent 4200 TapeStation. After removing the ribosomal RNA using the Epicentre Ribo-Zero Gold Kit (Illumina, San Diego, USA), the remaining RNA was fragmented using divalent cations under elevated temperature. The library construction was performed using the Hieff NGS® Ultima Dual-mode mRNA Library Prep Kit (Yeasen, Shanghai, China). The first strand of cDNA was synthesized in the 1st Strand Enzyme reverse transcriptase system using the fragmented RNA as the template and random oligonucleotides as the primer. Then 2nd Strand Enzyme and dUTPs were used to synthesize the second strand of cDNA. The purified double-stranded cDNA was end-repaired, A-tailed and ligated to the sequencing adapters. Finally, PCR amplification was performed to obtain the final sequencing library. Illumina Hiseq4000 was used for sequencing after quality inspection with the average insert size of 150 bp for the paired-end libraries. Quality control was carried out on the raw data obtained by sequencing. After removing the adaptor-polluted reads, low-quality reads and the reads with N bases accounting for >5 % of total bases, the filtered clean data was subjected to statistical analyses for quantity and quality. Quality control of clean data was performed by evaluating Q20 ($\geq$99 % base call accuracy), Q30 ($\geq$99.9 % accuracy) and GC content (the percentage of the total number of bases of G and C).

2.3. Transcript assembly and lncRNA identification

The reference genome and the annotation file of *A. japonicus* were used [19]. STAR software was used to map the clean data to the reference genome [35]. The mapped reads of each sample were assembled by StringTie (v2.2.1). The assembled transcripts were annotated using gffcompare (v0.12.8) to screen out known transcripts. The unknown transcripts were screened for putative lncRNAs. New transcripts with length >200 bp and exons ≥ 2 were candidate lncRNAs. Subsequently, Coding Potential Calculator 2 (CPC2), Coding-Non-Coding-Index (CNCI) and Predictor of Long non-coding RNAs and messenger RNAs based on an Improved k-mer Scheme (PLEK) were combined to predict the coding potential of the candidate lncRNAs and obtain the score value. By default, score <0 is considered to be non-coding, and score >0 is considered to have coding ability. Potential novel lncRNAs were filtered out by combining the three results. The lncRNAs were classified as Long intergenic non-coding RNA (lincRNAs), intronic lncRNAs, antisense lncRNAs, or sense lncRNAs according to the class code of "u", "i", "x", "o" by gffcompare.

2.4. Quantitation and differential lncRNA expression analysis

StringTie (v2.2.1) was used to quantify and FPKM (Fragments Per Kilobase per Million) values were calculated to quantify expression

levels. The lncRNAs differential expression analysis was performed by edgeR (v3.40.2) [36]. For the screening of differentially expressed lncRNAs (DE-lncRNAs), $|\log2(\text{FoldChange})| > 1$ (two-fold difference) and P value < 0.05 were assigned as significantly differentially-expressed.

2.5. Target gene prediction and functional analysis of lncRNA

LncRNAs regulate target genes through multiple mechanisms, primarily categorized as *cis*- or *trans*-acting [37,38]. In our study, cis-targeted genes are predicted based on the position between lncRNA and adjacent coding genes, also known as co-location target. Potential cis-targeted genes connected to lncRNAs were those found within a 100 kb flanking sequence, either upstream or downstream. Trans-targeted genes were predicted based on the correlation of expression levels by Pearson correlation coefficient, also known as co-expression target. For each lncRNA-mRNA pair, the Pearson correlation coefficient and *p*-value were calculated, with thresholds set at $|r| > 0.9$ and $p < 0.05$ for significance. Subsequently, Gene Ontology (GO) enrichment and Kyoto Encyclopedia of Genes and Genomes (KEGG) signaling-pathway analysis of the targeted genes were conducted using topGO (v2.50.0) [39] with Fisher's Exact Test as the statistical test and clusterProfiler (v4.6.2) [40] with Hypergeometric Test as the statistical test, respectively.

2.6. Secondary structure prediction and interaction network construction

We used Mfold online tool (http://www.unafold.org/mfold/applications/rna-folding-form.php) [41] to predict the secondary structure of lncRNAs with a false discovery rate (FDR) < 0.05, using default parameters. Similarly, for these lncRNAs, we performed lncRNA-miRNA interaction prediction using microRNA data [21] at miRanda v3.3a with Score Threshold 150 and Energy Threshold -20 kcal/mol. The interaction network between lncRNA and trans-targeted genes and the lncRNA-miRNA network were constructed using Cytoscape 3.9.3 software.

2.7. Validation by quantitative real-time PCR (qRT-PCR)

We randomly selected six DE-lncRNAs with significant differences for gene expression detection to evaluate the accuracy of sequencing. Total RNA was isolated using TaKaRa MiniBEST Universal RNA Extraction Kit (9767, Takara) and then reversed to cDNA with the random primer using a PrimeScript RT reagent Kit with gDNA Eraser (RR047A, Takara). Quantitative real-time PCR (qRT-PCR) was performed using SYBR® Premix ExTaq™ (RR820A, Takara). Primers used for DE-lncRNAs were designed at https://www.sangon.com/primerDesign and listed in Table S1. In the present study, three biological replicates (each with three technical replicates) were used for detection in each group. NADH dehydrogenase was used as a reference gene. The reaction system was carried out according to the steps of predenaturation, amplification cycle and melting curve. The specific reaction temperature and time were referred to previous article [16]. The relative expression level was measured using the $2^{-\Delta\Delta Ct}$ method. All data were analyzed by T-test in GraphPad Prism version9.0.0 for Windows (GraphPad Software, United States Massachusetts Boston, www.graphpad.com) and presented as mean ± SEM.

2.8. Dual-luciferase reporter assay

The lncRNA sequence containing the binding sites and the mutated sequence were synthesized and inserted into the pSI-Check2 luciferase reporter vector (Hanbio Biotechnology, China). The plasmids and miRNA mimics were co-transfected into HEK293T cells. A Dual-Luciferase Reporter Assay Kit (HB-DLR-100, HANBIO) was used to detect interaction. Finally, Renilla luciferase/firefly luciferase activity (R/F) was calculated to evaluate the combination.

3. Results

3.1. Identification and characterization of lncRNAs

To identify lncRNAs associated with intestinal regeneration in *A. japonicus*, six cDNA libraries from three control (Control_1, Control_2, Control_3) and three regenerated (3dpe_1, 3dpe_2, 3dpe_3) intestines were constructed. The clean nucleotide sequence data ranged from 10.29 to 13.58 Gb, and the data were submitted to the NCBI SRA database (accession number: PRJNA1196369). The Q30 scores exceeded 95 % across all samples (Table S2). After the transcripts were identified by CPC2, CNCI and PLEK, a total of 2361 lncRNAs were detected from the six samples (Fig. 1A). LncRNAs were classified into four categories based on genomic origin: lincRNAs (1652, 69.97 %), antisense-lncRNAs (248, 10.50 %), intronic-lncRNAs (416, 17.62 %) and sense-lncRNAs (45, 1.90 %) (Fig. 1B). All identified lncRNAs were novel and were designated with the prefix *MSTRG* [42]. We characterized these novel lncRNAs by assessing transcript lengths and exon numbers. Most of them were shorter than 3000 nucleotides, with 60.86 % under 1000 nucleotides (Fig. 1C). Nearly all lncRNAs contained ≤ 6 exons, with 90.34 % exhibiting 2 (72.85 %) or 3 (17.49 %) exons (Fig. 1D).

3.2. DE-lncRNAs during intestinal regeneration and lncRNA-mRNA regulation analysis

3.2.1. Differential expression of lncRNAs and Verification of lncRNA expression level

Compared with the control group, a total of 183 DE-lncRNAs were identified in regenerated intestines at 3dpe using the FPKM value, including 80 up-regulated DE-lncRNAs and 103 down-regulated DE-lncRNAs. The detailed information of DE-lncRNAs could be found in Table S3. Volcano plot (Fig. 2A) and circular heatmap (Fig. 2B) were generated to illustrate the overall distribution of DE-lncRNAs. The top five significantly up-regulated lncRNAs were MSTRG.18680, MSTRG.14360, MSTRG.14380, MSTRG.17922, and MSTRG.14751, while the top five significantly down-regulated lncRNAs were MSTRG.18440, MSTRG.6200, MSTRG.1184, MSTRG.14800, and MSTRG.5426 (Table 1).

To validate the RNA sequencing results, qRT-PCR was performed to verify the expression of lncRNAs. We selected the six lncRNAs for validation, which exhibited expression at each treatment and demonstrated the most significant differential expression. The results indicated that the trends observed in qRT-PCR were generally consistent with those from RNA-seq, although some differences did not reach statistical significance due to considerable individual variations among biological samples (Fig. 3).

3.2.2. Cis-targeted gene prediction

Cis-acting lncRNAs regulate local gene expression in a manner dependent on the location of their own sites of transcription. Functional enrichment analysis was conducted for *cis*-regulated target genes of lncRNAs. GO analysis revealed significant enrichment in biological process such as lipoprotein lipase regulation and vasculature development. In the cellular component category, the significantly enriched terms were primarily associated with extracellular matrix components, such as fibrinogen and tenascin. Terms related to substance binding, enzyme activity, and inhibitor activity were significantly enriched in the molecular function category (Fig. 4A). The KEGG results indicated that multiple signaling pathways related to cell adhesion and immunity were significantly enriched (Fig. 4B). The GO and KEGG enrichment results for the up-regulated and down-regulated genes cis-regulated by lncRNAs were presented in Figure S1. Compared with the control group, 62 differentially expressed lncRNAs could cis-regulate 67 differentially expressed target genes. A strong positive correlation was observed

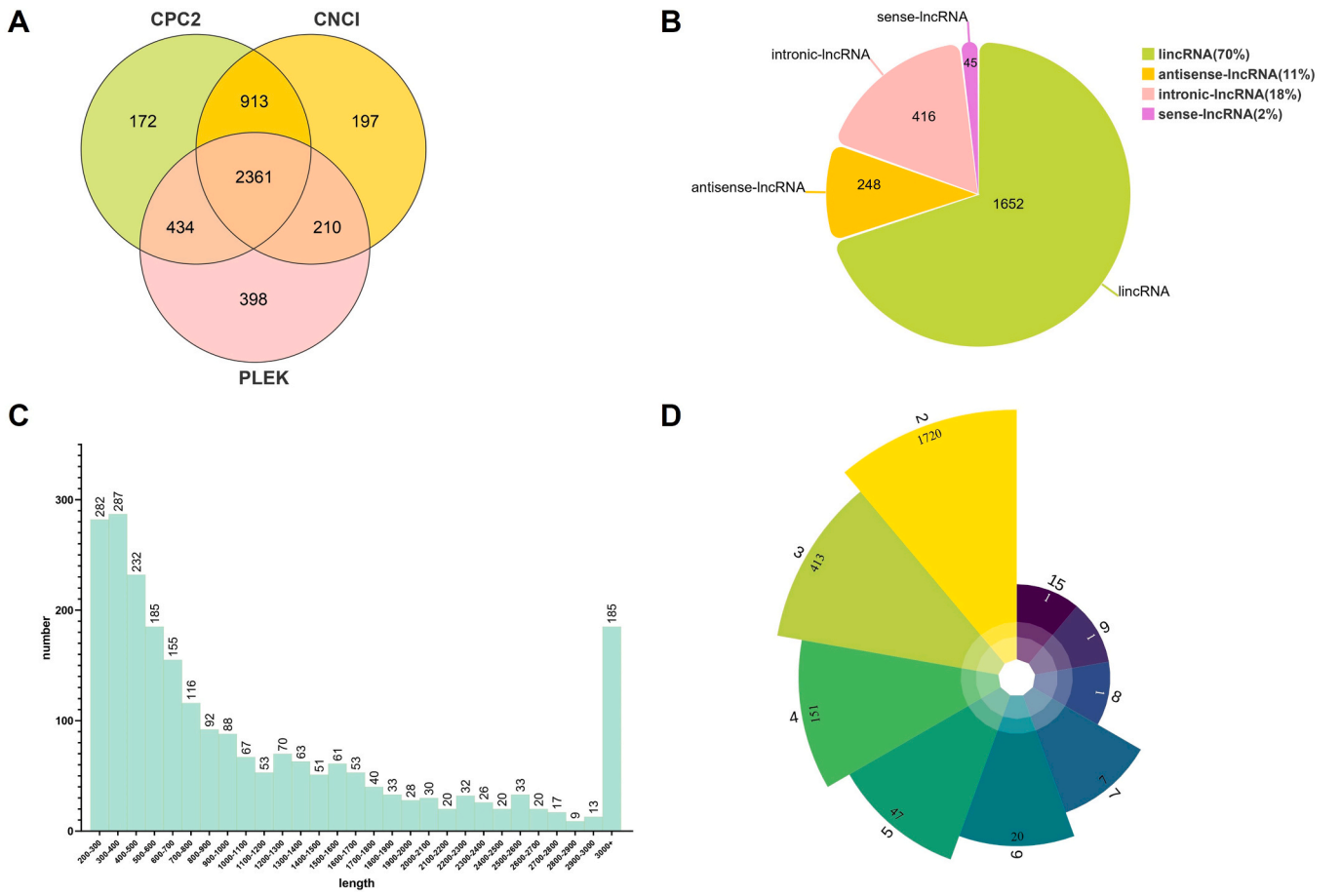

Fig. 1. Identification and characterisation of novel lncRNAs expressed in intestines during regeneration. A. Venn diagram showing lncRNAs identified by three tools (CPC2, CNCI, PLEK); B. Classification of the lncRNA according to the source; C. Distribution of novel lncRNAs based on length; D. Distribution of novel lncRNAs based on exon number.

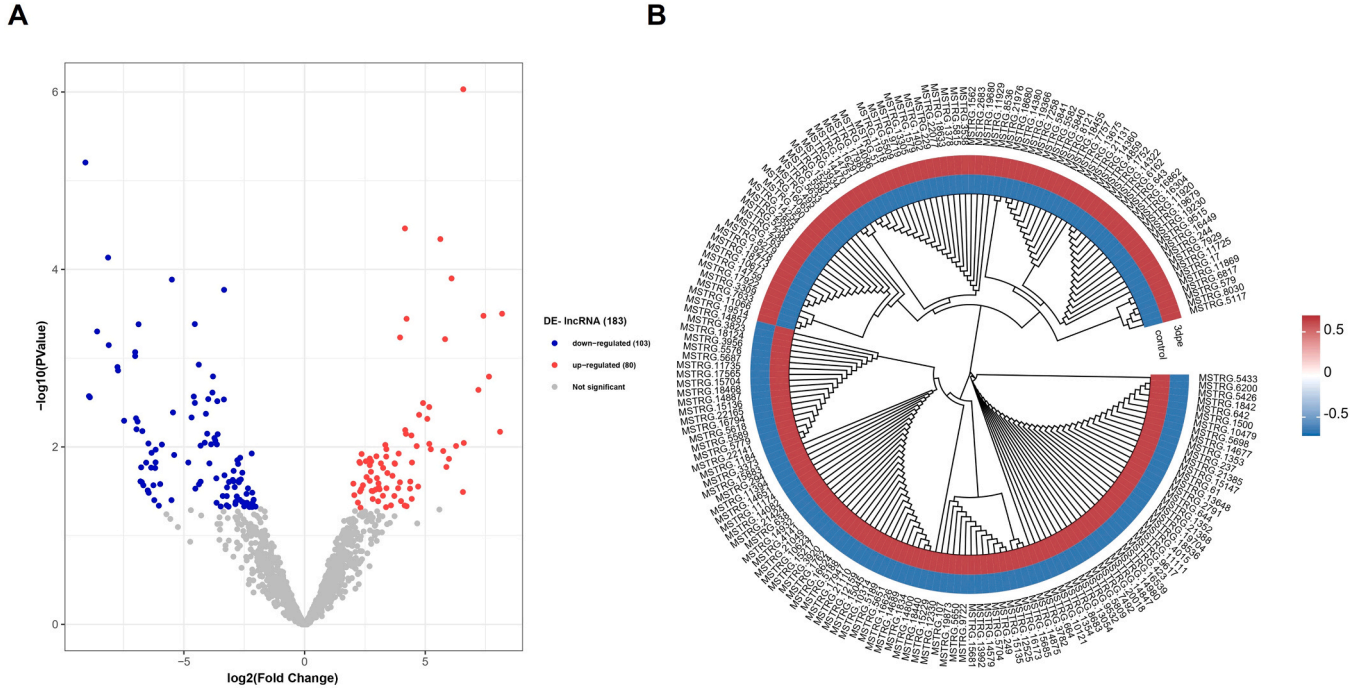

Fig. 2. Differentially expressed lncRNAs at 3dpe. A. Volcano plot analysis of DE-lncRNAs; B. The heatmap for DE-lncRNAs.

Table 1
The top 5 significantly up- and down-regulated lncRNAs at 3dpe during intestinal regeneration.

	lncRNA	logFC	PValue	position
up	MSTRG.18680	6.574479175	9.32E−07	Chr6: 25201830–25207140;-
	MSTRG.14360	4.159099409	3.45E−05	Chr3: 618757–723104;-
	MSTRG.14380	5.624907776	4.55E−05	Chr3: 1383397–1385916;-
	MSTRG.17922	6.088813307	0.000126192	Chr6: 3036390–3039976;+
	MSTRG.14751	8.182591357	0.000315278	Chr3: 14011171–14323172;+
down	MSTRG.18440	−9.079269195	6.23E−06	Chr6: 19458117–19461130;+
	MSTRG.6200	−8.140151011	7.35E−05	Chr14: 26378465–26379221;-
	MSTRG.1184	−5.496710555	0.000130113	Chr1: 33634388–33639872;-
	MSTRG.14800	−3.334540565	0.000169643	Chr3: 15636101–15687931;-
	MSTRG.5426	−4.546037889	0.000412711	Chr14: 7845942–7871537;+

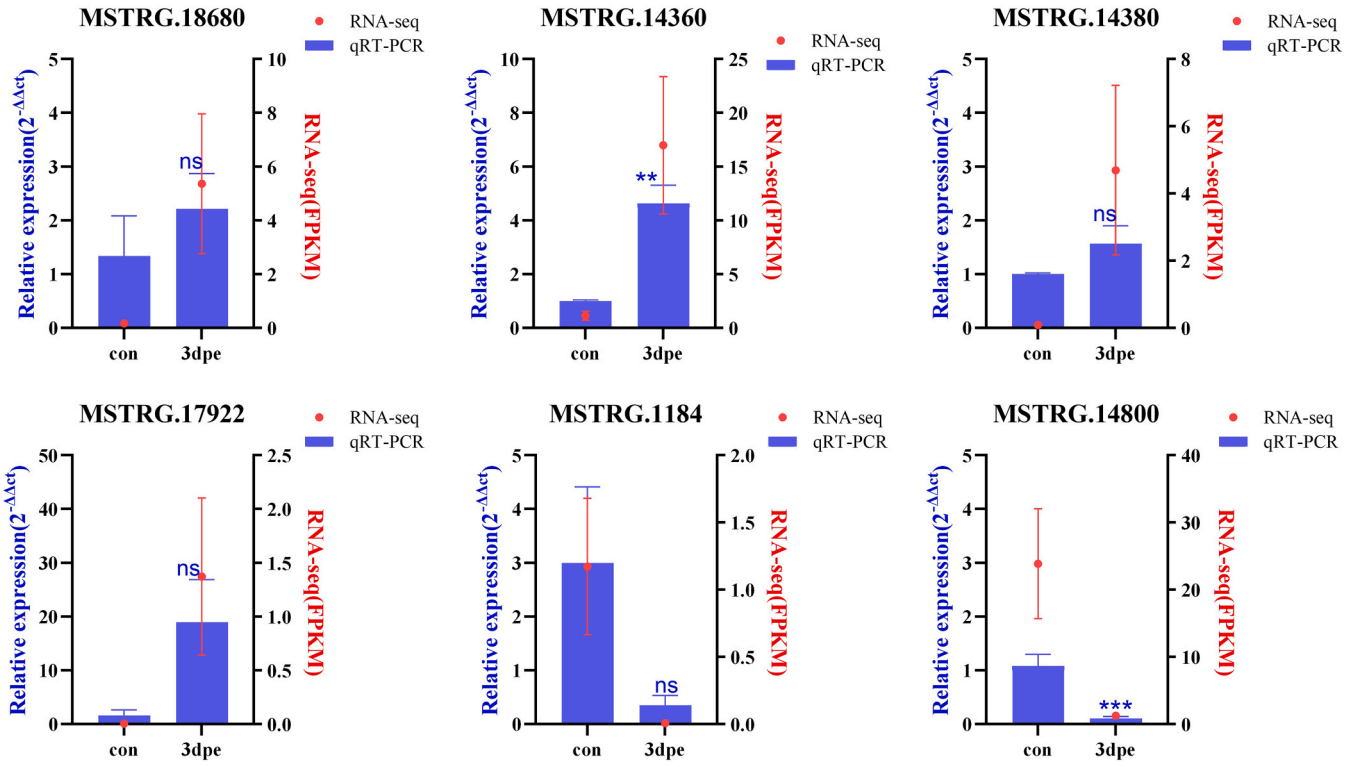

Fig. 3. Validation of the six lncRNAs by qRT-PCR. NADH was selected to normalize the gene expression levels. The data are shown as means (± SE) of at least three replicates. Red bars: Significantly differentially expressed lncRNAs in RNA-seq (|log2FC= >1, $p < 0.05$); Blue bars: RT-qPCR-validated lncRNAs (Student's *t*-test, ** $p < 0.01$,*** p < 0.001, ns no significance).

between DE-lncRNAs and their *cis*-target mRNAs. Among these predictions, seven target genes were annotated in the genome, and these results were detailed in Table 2. Notably, two immune-related genes (*Ficolin-1*, *fibrinogen-like protein A-like*) and an oxidative stress-associated gene (*lactoperoxidase-like*) were identified. This is also consistent with the KEGG enrichment results.

3.2.3. *Trans-targeted gene prediction and lncRNA-mRNA co-expression network construction*

A co-expression relationship was defined as having a Pearson correlation coefficient |r| > 0.9 for lncRNA-mRNA pairs. Genes exhibiting co-expression relationships were subjected to functional enrichment analysis (Fig. 5A, B). In the biological process category of GO, several terms associated with stimulus response exhibited significant enrichment, along with two terms related to phosphorus metabolism. In the cellular component category, multiple vesicle-related terms and extracellular component terms were significantly enriched. In the molecular function category, terms related to ion binding and kinase binding demonstrated significantly enriched (Fig. 5A). The KEGG enrichment results showed that multiple co-expressed genes were significantly enriched in the PI3K-Akt and Rap1 signaling pathways. Signaling pathways involved in energy metabolism, including carbon metabolism, lipid metabolism, and glycolysis, were also significantly enriched (Fig. 5B). The GO and KEGG enrichment results for the up-regulated and down-regulated genes trans-regulated by lncRNAs were presented in Figure S2.

A lncRNA-mRNA co-expression network was constructed using DE-lncRNAs and their trans-targeted DE-mRNAs (Fig. 5C). The network contained 117 mRNAs and 191 lncRNAs. A single lncRNA could trans-regulate multiple mRNAs, while an mRNA could also be trans-regulated by several lncRNAs simultaneously. The network predominantly displayed positive regulatory interactions, with the exception of MSTRG.763 demonstrating negative regulation of three target genes.

3.3. *LncRNAs as endogenous target mimics for miRNAs*

Compared to mRNAs, a distinctive feature of lncRNAs is their tendency to fold into secondary and tertiary structures, providing abundant binding sites for interactions with other molecules, such as miRNAs and transcription factors [43]. We predicted the secondary structures of

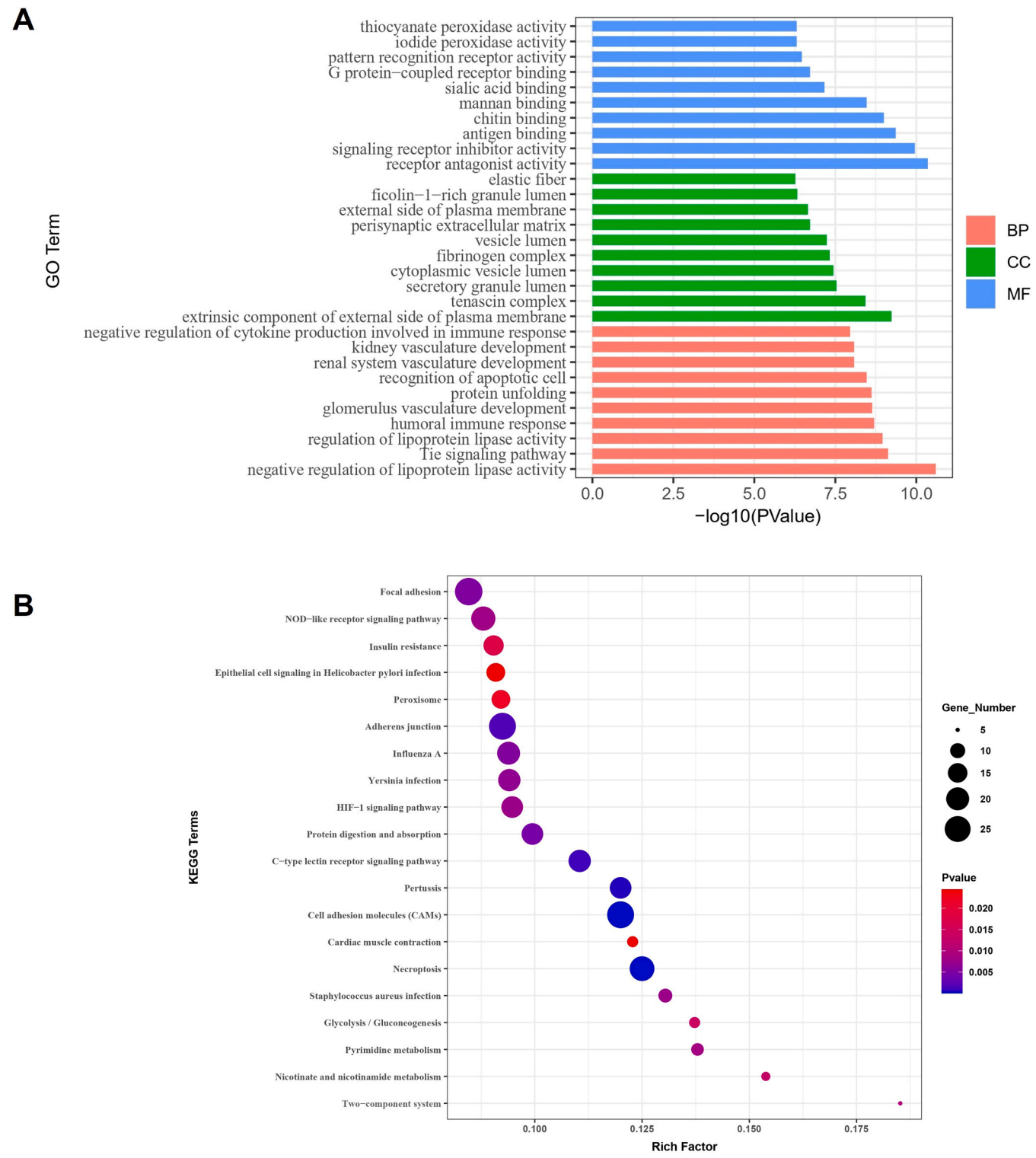

Fig. 4. Enrichment analysis of cis-targeted genes. A. Gene Ontology (GO) enrichment of cis-targeted genes. Categories: Biological Process (BP), Cellular Component (CC), and Molecular Function (MF); B. Kyoto Encyclopedia of Genes and Genomes (KEGG) enrichment of cis-targeted genes.

MSTRG.1184, MSTRG.6200, MSTRG.14360, MSTRG.14380, MSTRG.17922, MSTRG.18440, and MSTRG.18680, all of which exhibited multiple stem-loop structures (Fig. 6).

Since lncRNAs can compete for miRNA-mediated inhibition by acting as a sponge for miRNA, leading to increased mRNA expression, we screened lncRNA-miRNA interacting pairs and constructed the interaction network by comprehensively evaluating the free energy required for lncRNA binding to miRNA and whether lncRNA has a sequence complementary to the seed region of miRNA (Fig. 7). Targeted miRNA predictions were performed for these seven lncRNAs, resulting in the identification of 137 predicted miRNAs. Each lncRNA contains multiple binding sites for miRNAs.

We analyzed the differential expression of these miRNAs at 3dpe. Among these, miR-7847–3p and miR-4220–5p were up-regulated, whereas miR-4214–5p was down-regulated [21]. According to the results of interaction prediction, three binding sites were identified

Table 2
Cis-regulated lncRNA-mRNA pairs whose target genes were annotated in the genome.

lncRNA	logFC	PValue	lnc_diffStat	targetGene	target_diffStat	targetGene_description
MSTRG.423	−6.79776	0.024472	down-regulated	evm.TU.Chr1.300	down-regulated	ATP-dependent DNA helicase PIF1 [*Holothuria leucospilota*]
MSTRG.2683	3.048642	0.040999	up-regulated	evm.TU.Chr11.122	up-regulated	putative sodium/glucose cotransporter 4 isoform X2 [*Apostichopus japonicus*]
MSTRG.3538	3.24642	0.035539	up-regulated	evm.TU.Chr11.891	up-regulated	lactoperoxidase-like [*Strongylocentrotus purpuratus*]
MSTRG.9515	2.75001	0.019065	up-regulated	evm.TU.Chr18.582	up-regulated	hypothetical protein BSL78_20370 [*Apostichopus japonicus*]
MSTRG.9532	−6.22679	0.039812	down-regulated	evm.TU.Chr18.582	up-regulated	hypothetical protein BSL78_20370 [*Apostichopus japonicus*]
MSTRG.14677	−7.75118	0.001257	down-regulated	evm.TU.Chr3.307	down-regulated	Ficolin−1 [*Rattus norvegicus*]
MSTRG.15135	−4.08724	0.004234	down-regulated	evm.TU.Chr3.638	down-regulated	putative fibrinogen-like protein A-like [*Apostichopus japonicus*]
MSTRG.21385	−5.45021	0.004089	down-regulated	evm.TU.Chr9.238	down-regulated	Protein Skeletor, isoforms B/C [*Drosophila melanogaster*]

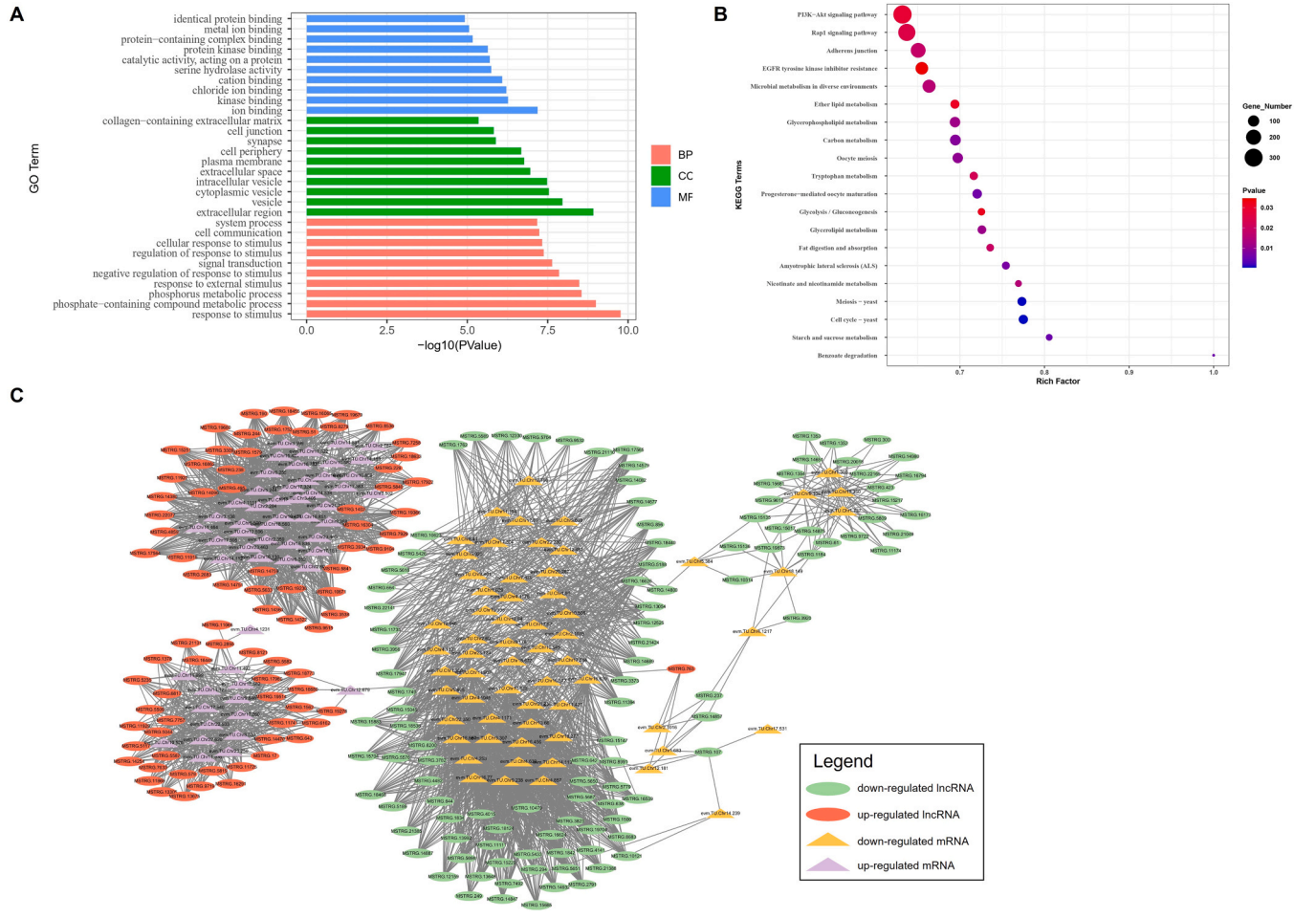

Fig. 5. Analysis of trans-targeted genes. A. Gene Ontology (GO) enrichment of trans-targeted genes; B. Kyoto Encyclopedia of Genes and Genomes (KEGG) enrichment of trans-targeted genes; C. The interaction network of DE-lncRNA and DE-mRNA.

between MSTRG.6200 and miR-7847–3p, two binding sites between MSTRG.14380 and miR-4214–5p, one binding site between MSTRG.18440 and miR-4220–5p (Fig. 8A-C).

To determine whether true binding exists, we conducted dual-luciferase reporter assays for these three lncRNA-miRNA pairs (Fig. 8D-F). We compared a luciferase plasmid containing the wild-type lncRNA sequence (with all identified binding sites) and a mutant plasmid with mutations introduced at all binding sites. We found that the R/F ratio in the group co-transfected with the miR-7847–3p mimic and the wild-type plasmid was significantly lower than that in the control group. However, the R/F ratio in the mutant plasmid group showed no significant difference from the control, thus, indicating that MSTRG.6200 has a valid binding site for miR-7847–3p. Similarly, the predicted binding site of MSTRG.18440 for miR-4220–5p was also effective. However, miR-4214–5p mimics did not suppress the luciferase reporter activity. Therefore, MSTRG.14380 cannot bind to miR-4214–5p.

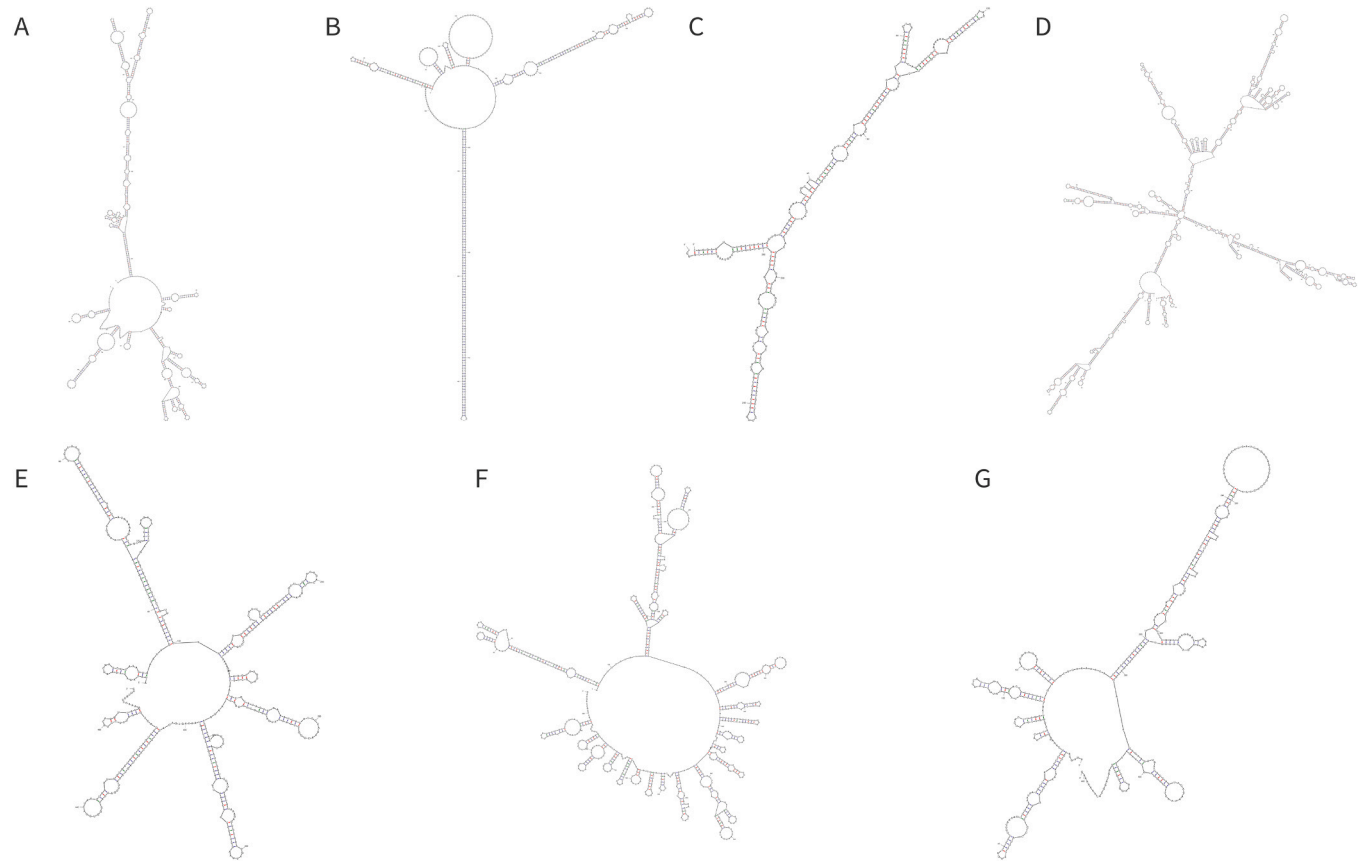

Fig. 6. Secondary structures of MSTRG.1184 (A), MSTRG.6200 (B), MSTRG.14360 (C), MSTRG.14380 (D), MSTRG.17922 (E), MSTRG.18440 (F), and MSTRG.18680 (G).

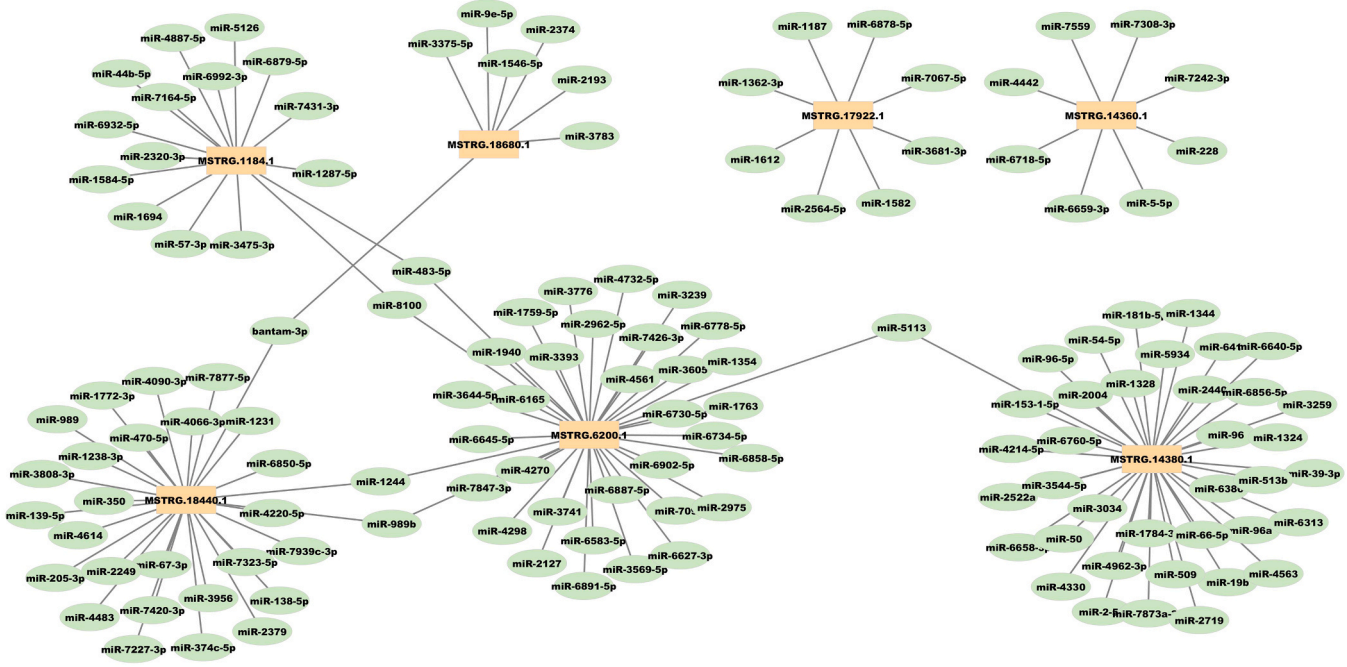

Fig. 7. The lncRNAs-miRNAs network of 7 candidate lncRNAs.

4. Discussion

In this study, transcriptome sequencing was employed to investigate the changes in lncRNA expression during intestinal regeneration in *A. japonicus*. A total of 2361 lncRNAs were identified, with 183 showing differential expression in the intestine at 3dpe, including 80 upregulated and 103 downregulated. Among them, some DE-lncRNAs are exclusively expressed in the normal intestine or solely in regenerating intestines

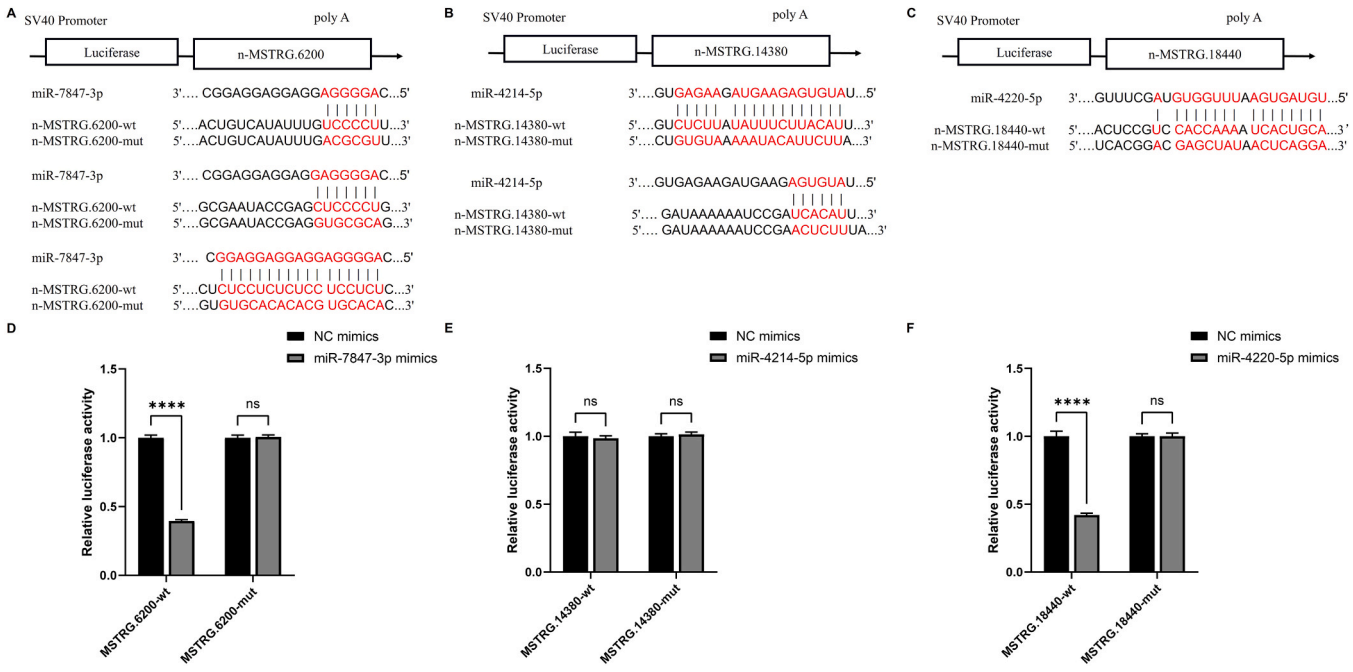

Fig. 8. Dual-luciferase assay reporter system results of lncRNA-miRNA. A-C. Schematic of target site combination for MSTRG.6200 and miR-7847–3p (A), MSTRG.14380 and miR-4214–5p (B), MSTRG.18440 and miR-4220–5p (C); D-F. The relative luciferase activities were investigated post co-transfection with lncRNA-wt or lncRNA-mut plasmids and modified miRNA mimics or NC mimics. NC mimics means negative control mimics. NC mimics: UUCUCCGAACGUGUCACGUdTdT * ** * $p < 0.0001$.

(Table S3), suggesting the specific involvement of lncRNAs in regulating gene expression during intestinal regeneration, and exhibiting distinct expression patterns [22,44].

At 3dpe, the regenerating intestine underwent diverse and pronounced physiological activities. Evisceration induced oxidative stress, leading to the production of reactive oxygen species (ROS) and the activation of various cellular antioxidant enzymes [8]. The organism maintained a high level of antioxidant capacity, even throughout the entire regeneration period [45]. Humoral immunity was also notably active and numerous factors and protective molecules were synthesized and released at 3dpe [8]. Meanwhile, energy accumulation in the esophagus remnant involved proteins related to amino acid transport and metabolism with reduced lipid transport [46,47]. Downregulation of genes associated with cell adhesion, particularly cadherins [48], was coordinated with the migration of coelomic epithelial cells [8]. During this period, extracellular matrix (ECM) was degraded and reconstituted, with several protease classes involved in the degradation of collagen fibrils [8,49,50], including matrix metalloproteinase (MMP-2, MMP-16) [51]. In our study, the genes regulated by lncRNAs via cis- or trans-targeting were all involved in several of the processes mentioned above. Both cis- and trans-targeted genes were enriched in GO terms associated with extracellular components. Downregulated cis-targeted genes were enriched in pathways related to cell adhesion, including adherens junctions, focal adhesion, and cell adhesion molecules (CAMs) signaling pathways (Fig. 4A, S1), consistent with the findings above. Trans-targeted genes were enriched in biological process terms associated with phosphate metabolism and were involved in signaling pathways related to energy metabolism, such as carbon and lipid metabolism (Fig. 5). Downregulated cis-targeted genes were enriched in biological process terms related to lipoprotein lipase activity, corresponding with reduction in lipid transport. Additionally, the target genes under cis-regulation were enriched in the peroxisome signaling pathway (Fig. 4B). The target gene lactoperoxidase-like (Table 2) is linked to oxidative stress [52], suggesting that lncRNAs play a role in oxidative stress responses during intestinal regeneration. The cis-targeted genes, Ficolin-1 and fibrinogen-like protein A-like (FGL1) (Table 2), were implicated in immune defense mechanisms [53–55]. The cis-targeted genes were enriched in immune signaling pathways, such as C-type lectin receptor signaling pathway (Fig. 4B), while the trans-targeted genes were predominantly associated with biological process terms related to stimulus response (Fig. 5A). The results suggested that lncRNAs are involved in the regulation of immune responses. In summary, these findings highlight the critical roles of lncRNAs in oxidative stress, immune response, extracellular matrix remodeling, and energy metabolism during intestinal regeneration.

LncRNAs can act as sponges for miRNAs and mitigate the inhibitory effects of miRNAs on target genes [56]. Here, we constructed a lncRNA-miRNA interaction network using previously published miRNA data [21]. We predicted miRNA interaction for the most significantly differentially expressed lncRNAs and mapped the interaction network. Through dual luciferase reporter assays, we confirmed that MSTRG.6200 and MSTRG.18440 indeed function as sponges for miR-7847–3p and miR-4220–5p, respectively. The negative correlation between lncRNA and miRNA is indicated by the upregulation of one and downregulation of the other, and vice versa. Thus, lncRNAs may participate in the regulation of intestinal regeneration in *A. japonicus* by acting as competing endogenous RNAs (ceRNAs). Additionally, studies have emphasized the significance of other lncRNA-miRNA-mRNA networks in sea cucumbers. The "HIF-1α gene/Aja-miR-2013–3p/MSTRG.34610" and the "HIF-1α gene/Aja--miR-2013–3p/MSTRG.10941" networks may play important roles in *A. japonicus* under environmental stresses [42]. These findings highlight the complexity and diversity of lncRNA-mediated regulatory mechanisms in sea cucumbers.

It has been speculated that miR-7847–3p and miR-4220–5p may target Fibrinogen-like protein A and Alpha tubulin, respectively [21]. Alpha tubulin is a member of cytoskeletal genes, which are highly expressed during cell growth. During intestinal regeneration at 3dpe, some of these genes increase in expression, while others decrease, dynamically regulating cell proliferation [16,57]. FGL1 is a secreted protein involved in the complement system, playing a key role in immune defense [55]. It may be cis-targeted by MSTRG.15135 and also serve as a target gene for miR-7847–3p, with its expression being

indirectly influenced by MSTRG.6200. Given these findings, further investigation of the regulatory networks involving miR-7847–3p, MSTRG.6200 and MSTRG.15135 is necessary to clarify their roles in modulating *FGL A* expression and its effect on immune defense.

5. Conclusion

In this study, we demonstrate, for the first time, the differential expression of lncRNAs during the early stage of intestinal regeneration in sea cucumber *A. japonicus*. We also constructed lncRNA–mRNA and lncRNA–miRNA interaction networks. A total of 183 DE-lncRNAs were identified. These lncRNAs regulate various processes in intestinal regeneration, including oxidative stress, immune response, extracellular matrix remodeling, and energy metabolism. The dual-luciferase assay revealed that MSTRG.6200 and MSTRG.18440 act as sponges for miR-7847–3p and miR-4220–5p, respectively. Our findings expand the lncRNA database of echinoderms and facilitate further investigations into the potential regulatory mechanisms underlying the lncRNA-mediated regeneration in animals. Our comprehensive study of regeneration in *A. japonicus* also provides insights for future research in regenerative medicine.

Author contributions

Hongsheng Yang and Lina Sun conceived the study. Fang Su carried out the laboratory work, participated in the data analysis, and drafted the manuscript. Igor Yu. Dolmatov conducted data analysis and manuscript revision. Tianming Wang, Kui Ding, and Libin Zhang revised the manuscript. All authors approved the manuscript for publication.

CRediT authorship contribution statement

Yang Hongsheng: Methodology, Investigation. **Ding Kui:** Writing – review & editing, Funding acquisition. **Zhang Libin:** Writing – review & editing. **Sun Lina:** Writing – review & editing, Funding acquisition, Conceptualization. **Su Fang:** Writing – original draft, Validation, Methodology. **Dolmatov Igor Yu.:** Writing – review & editing, Conceptualization. **Wang Tianming:** Writing – review & editing, Methodology.

Declaration of Competing Interest

The authors declare that they have no known competing financial interests or personal relationships that could have appeared to influence the work reported in this paper.

Acknowledgments

This work was supported by the National Natural Science Foundation of China [grant number No. 42276143, 42076093, 42106131], Shandong Provincial Natural Science Foundation [grant number No. ZR2024YQ050] and Taishan Scholar Foundation of Shandong Province [grant number No. 202306279].

Appendix A. Supporting information

Supplementary data associated with this article can be found in the online version at doi:10.1016/j.csbj.2025.03.047.

References

[1] Bourlat SJ, Juliusdottir T, Lowe CJ, Freeman R, Aronowicz J, Kirschner M, et al. Deuterostome phylogeny reveals monophyletic chordates and the new phylum Xenoturbellida. Nature 2006;444(7115):85–8.
[2] Gahn FJ, Baumiller TK. Evolutionary history of regeneration in crinoids (Echinodermata). Integr Comp Biol 2010;50(4). 514-514.
[3] Emson RH, IC W. Fission and autotomy in echinoderms. Oceano Mar Biol Annu Rev 1980;18:155–250.
[4] Dolmatov IY. Variability of regeneration mechanisms in echinoderms. Russ J Mar Biol 2020;46(6):391–404.
[5] Mashanov V, García-Arrarás J. Gut regeneration in holothurians: a snapshot of recent developments. Biol Bull 2011;221(1):93–109.
[6] Quispe-Parra D, Valentin G, Garcia-Arraras JE. A roadmap for intestinal regeneration. Int J Dev Biol 2020.
[7] Medina-Feliciano JG, Garcia-Arraras JE. Regeneration in echinoderms: molecular advancements. Front Cell Dev Biol 2021;9:768641.
[8] Dolmatov IY. Molecular aspects of regeneration mechanisms in holothurians. Genes 2021;12(2):250.
[9] Su F, Yang H, Sun L. A review of histocytological events and molecular mechanisms involved in intestine regeneration in holothurians. Biology 2022;11(8).
[10] Shukalyuk A, Dolmatov IY. Regeneration of the digestive tube in the holothurian *Apostichopus japonicus* after Evisceration. Russ J Mar Biol 2001;27(3):168–73.
[11] Wang X, Li X. The morphological and histological observation of regeneration of alimentary tract in sea cucumber *Apostichopus japonicus*. J Dalian Fish Univ 2007; 22(5):340–6.
[12] Zeng C, Guo M, Xiang Y, Song M, Xiao K, Li C. Mesentery AjFGF4-AjFGFR2-ERK pathway modulates intestinal regeneration via targeting cell cycle in echinoderms. Cell Prolif 2022:e13351.
[13] Garcia-Arraras JE, Bello SA, Malavez S. The mesentery as the epicenter for intestinal regeneration. Semin Cell Dev Biol 2019;92:45–54.
[14] Mashanov VS, Dolmatov IY, Heinzeller T. Transdifferentiation in holothurian gut regeneration. Biol Bull 2005;209(3):184.
[15] García-Arrarás J, Estrada-Rodgers L, Santiago R, Torres II, Díaz-Miranda L, Torres-Avillán I. Cellular mechanisms of intestine regeneration in the sea cucumber, *Holothuria glaberrima* Selenka (Holothuroidea: Echinodermata). J Exp Zool 1998; 281(4):288–304.
[16] Su F, Dolmatov IY, Cui W, Yang H, Sun L. Molecular dynamics and spatial response of proliferation and apoptosis in wound healing and early intestinal regeneration of sea cucumber *Apostichopus japonicus*. Dev Comp Immunol 2024;162:105297.
[17] Cech TR, Steitz JA. The noncoding RNA revolution-trashing old rules to forge new ones. Cell 2014;157(1):77–94.
[18] Zhang X, Sun L, Yuan J, Sun Y, Gao Y, Zhang L, et al. The sea cucumber genome provides insights into morphological evolution and visceral regeneration. PLOS Biol 2017;15(10):e2003790.
[19] Sun L, Jiang C, Su F, Cui W, Yang H. Chromosome-level genome assembly of the sea cucumber *Apostichopus japonicus*. Sci Data 2023;10(1).
[20] Su F, Huo D, Yang H, Sun L. CircRNA8388 functions as the sponge for miR-2392 during intestinal regeneration in sea cucumber *Apostichopus japonicus*. Int J Biol Macromol 2024;274.
[21] Sun L, Sun J, Li X, Zhang L, Yang H, Wang Q. Understanding regulation of microRNAs on intestine regeneration in the sea cucumber *Apostichopus japonicus* using high-throughput sequencing. Comp Biochem Physiol Part D Genom Proteom 2017;22:1–9.
[22] Mallory AC, Shkumatava A. LncRNAs in vertebrates: advances and challenges. Biochimie 2015;117:3–14.
[23] Zhang S, Shao Y, Li C. Characterization of Host lncRNAs in response to vibrio splendidus infection and function as efficient miRNA sponges in sea cucumber. Front Immunol 2021;12:792040.
[24] Huang XD, Dai JG, Lin KT, Liu M, Ruan HT, Zhang H, et al. Regulation of IL-17 by lncRNA of IRF-2 in the pearl oyster. Fish Shellfish Immunol 2018;81:108–12.
[25] Chen J, Wang Y, Wang C, Hu J-F, Li W. LncRNA functions as a new emerging epigenetic factor in determining the fate of stem cells. Front Genet 2020;11.
[26] Novikova IV, Hennelly SP, Tung CS, Sanbonmatsu KY. Rise of the RNA machines: exploring the structure of long non-coding RNAs. J Mol Biol 2013;425(19): 3731–46.
[27] Camilleri-Robles C, Amador R, Tiebe M, Teleman AA, Serras F, Guigo R, et al. Long non-coding RNAs involved in Drosophila development and regeneration. NAR Genom Bioinform 2024;6(3):lqae091.
[28] Liu H, Liu H, Yang Q, Fan Z. LncRNA SNHG1 enhances cartilage regeneration by modulating chondrogenic differentiation and angiogenesis potentials of JBMMSCs via mitochondrial function regulation. Stem Cell Res Ther 2024;15(1):177.
[29] Wu X, Shen T, Ji W, Huang M, Sima J, Li J, et al. lncRNA CASC11 regulates the progress of delayed fracture healing via sponging miR-150-3p. J Orthop Surg Res 2024;19(1).
[30] Yadav VK, Kumar A, Tripathi PP, Gupta J. Long noncoding RNAs in intestinal homeostasis, regeneration, and cancer. J Cell Physiol 2021;236(11):7801–13.
[31] Xu Q, Liu J, Du X, Xue D, Li D, Bi X. Long non-coding RNA CR46040 is essential for injury-stimulated regeneration of intestinal stem cells in Drosophila. Genetics 2023.
[32] Geng H, Bu HF, Liu F, Wu L, Pfeifer K, Chou PM, et al. In inflamed intestinal tissues and epithelial cells, interleukin 22 signaling increases expression of H19 long noncoding RNA, which promotes mucosal regeneration. Gastroenterology 2018; 155(1):144–55.
[33] Deng Q, Zhao N, Zhu C, Zhang B. Long non-coding RNAs in the physiology of aquaculture animals: a perspective update. Rev Fish Biol Fish 2022;32(4):1103–22.
[34] Mercer TR, Dinger ME, Mattick JS. Long non-coding RNAs: insights into functions. Nat Rev Genet 2009;10(3):155–9.
[35] Dobin A, Davis CA, Schlesinger F, Drenkow J, Zaleski C, Jha S, et al. STAR: ultrafast universal RNA-seq aligner. Bioinformatics 2013;29(1):15–21.
[36] Robinson MD, McCarthy DJ, Smyth GK. edgeR: a bioconductor package for differential expression analysis of digital gene expression data. Bioinformatics 2010;26(1):139–40.

[37] Xu W-H, Zhang J-B, Dang Z, Li X, Zhou T, Liu J, et al. Long non-coding RNA URHC regulates cell proliferation and apoptosis via ZAK through the ERK/MAPK signaling pathway in hepatocellular carcinoma. Int J Biol Sci 2014;10(7):664–76.
[38] Li Y, Zhang C, Qin L, Li D, Zhou G, Dang D, et al. Characterization of critical functions of long non-coding RNAs and mRNAs in rhabdomyosarcoma cells and mouse skeletal muscle infected by enterovirus 71 using RNA-Seq. Viruses 2018;10 (10).
[39] Yang X, Liu C, Niu X, Wang L, Li L, Yuan Q, et al. Research on lncRNA related to drought resistance of Shanlan upland rice. BMC Genom 2022;23(1):336.
[40] Yu G, Wang LG, Han Y, He QY. clusterProfiler: an R package for comparing biological themes among gene clusters. OMICS 2012;16(5):284–7.
[41] Zuker M. Mfold web server for nucleic acid folding and hybridization prediction. Nucleic Acids Res 2003;31(13):3406–15.
[42] Huo D, Sun L, Storey KB, Zhang L, Liu S, Sun J, et al. The regulation mechanism of lncRNAs and mRNAs in sea cucumbers under global climate changes: defense against thermal and hypoxic stresses. Sci Total Environ 2020;709:136045.
[43] Graf J, Kretz M. From structure to function: route to understanding lncRNA mechanism. BioEssays 2020;42(12).
[44] Han P, Chang CP. Long non-coding RNA and chromatin remodeling. RNA Biol 2015;12(10):1094–8.
[45] Zang Y, Tian X, Dong S, Dong Y. Growth, metabolism and immune responses to evisceration and the regeneration of viscera in sea cucumber *Apostichopus japonicus*. Aquaculture 2012;358:50–60.
[46] Sun L, Xu D, Xu Q, Sun J, Xing L, Zhang L, et al. iTRAQ reveals proteomic changes during intestine regeneration in the sea cucumber *Apostichopus japonicus*. Comp Biochem Physiol Part D Genom Proteom 2017;22:39–49.
[47] Sun L, Lin C, Li X, Xing L, Huo D, Sun J, et al. Comparative phospho- and acetyl proteomics analysis of posttranslational modifications regulating intestine regeneration in sea cucumbers. Front Physiol 2018;9:836.
[48] Quispe-Parra DJ, Medina-Feliciano JG, Cruz-Gonzalez S, Ortiz-Zuazaga H, Garcia-Arraras JE. Transcriptomic analysis of early stages of intestinal regeneration in *Holothuria glaberrima*. Sci Rep 2021;11(1):346.
[49] Dolmatov IY, Afanasyev SV, Boyko AV. Molecular mechanisms of fission in echinoderms: transcriptome analysis. PLOS ONE 2018;13(4):e0195836.
[50] Dolmatov IY, Nizhnichenko VA. Extracellular matrix of echinoderms. Mar Drugs 2023;21(7).
[51] Miao T, Wan Z, Sun L, Li X, Xing L, Bai Y, et al. Extracellular matrix remodeling and matrix metalloproteinases (ajMMP-2 like and ajMMP-16 like) characterization during intestine regeneration of sea cucumber *Apostichopus japonicus*. Comp Biochem Physiol Part B Biochem Mol Biol 2017;212:12–23.
[52] Panizzolo M, Martins VH, Ghelli F, Squillacioti G, Bellisario V, Garzaro G, et al. Biomarkers of oxidative stress, inflammation, and genotoxicity to assess exposure to micro- and nanoplastics. A literature review. Ecotoxicol Environ Saf 2023;267: 115645.
[53] Zhang L, Feng Q, Sun L, Ding K, Huo D, Fang Y, et al. Differential gene expression in the intestine of sea cucumber (*Apostichopus japonicus*) under low and high salinity conditions. Comp Biochem Physiol Part D Genom Proteom 2018;25:34–41.
[54] Jiang J, Gao S, Wang X, Guan X, Wang B, Chen Z, et al. The role of a novel secretory peptidoglycan recognition protein from the sea cucumber *Apostichopus japonicus* in innate immunity. Aquaculture 2022;546.
[55] Wang J, Sanmamed MF, Datar I, Su TT, Ji L, Sun J, et al. Fibrinogen-like Protein 1 Is a Major Immune Inhibitory Ligand of LAG-3. Cell 2019;176(1-2):334–47. e12.
[56] Militello G, Weirick T, John D, Doring C, Dimmeler S, Uchida S. Screening and validation of lncRNAs and circRNAs as miRNA sponges. Brief Bioinform 2017;18 (5):780–8.
[57] Sun L, Yang H, Chen M, Ma D, Lin C. RNA-Seq reveals dynamic changes of gene expression in key stages of intestine regeneration in the sea cucumber *Apostichopus japonicus*. Plos One 2013;8(8):e69441.